Strain rate analysis over the Central Apennines from GPS velocities: the development of a new free software.

Arianna Pesci (1), Giordano Teza (2)

(1) INGV, Sezione di Bologna, via Creti 12, Bologna (Italy).

(2) Dipartimento di Geologia, Palentologia e Geofisica,Università degli Studi di Padova, Via Giotto, 1 - 35137 Padova (Italy).

Abstract

Displacements or velocities obtained by GPS data processing over repeated surveys can provide useful information on tensional states of terrestrial crust, in those areas in which many stations well spatially distributed are present. In particular, the strain (or strain rate) can be computed over the nodes of a regular grid with suitable size to define a high density deformation field.
A new method was deployed to generate easily and quickly the deformation pattern from GPS velocities and to evaluate the significance: values, related to an assigned grid point, can be truly considered only if the GPS stations are well distributed around it. The approach validation was performed by means of synthetic data derived from the theoretical displacement field generated by a Mogi model source.
A complete analysis on the velocity pattern of the CaGeoNet network (Central Apennine chain, Italy) was performed providing strain rates and showing both extensional and compressive behaviour at the same values, along the Appennine chain axis.

Key-words: GPS, CAGeoNet, velocity, strain, continuous.

Introduction

The GPS data are collected and processed in order to provide station coordinates within a few millimeters' accuracy. The networks characterized by a high density point distribution, rarely allows the installation of permanent stations for a continuous monitoring on all vertices, but can provide a very interesting sub-regional and detailed study of the area by means of repeated surveys. In a previous study, Anzidei et al. (2005) estimated for the first time a significant compressive strain along the Central Apennine chain, from the CaGeoNet network data. The network extends from Tyrrhenian to Adriatic coasts, and the distribution of stations in the middle is very dense, with a mean relative distance of a few kilometers.
In order to provide consistent results, independent from the choice of the reference frame, a strain rate estimation was performed through the development of a new software (the `grid_strain` Matlab™ program). It allows the definition of a deformation pattern with a chosen spatial distribution in the whole area over a regular grid. Several routines are applied during computation to accept or exclude local estimates at nodes around which GPS data points can be poorly distributed from the geometrical point of view. In the next paragraphs a complete and detailed application is described and results are analyzed to provide detailed kinematics of the investigated area.

Theoretical aspect and approach validation

Within a continuous material it is possible to define mathematical relationships between displacement (or velocities) and the acting deformation (or deformation rate). Introducing the 2D spatial displacement gradient **L** (L_{ij}) and free to choose a convenient reference system, planimetric movements around a point are given, at the first order as: $u_i = L_{ij} dx_j + U_i$, where U_i are constants and dx_j the infinitesimal increment along x and y axes. The gradient tensor

($L_{ij} = u_{i,j}$) can be separated in two parts $\mathbf{L} = \mathbf{E} + \mathbf{\Omega}$ ($L_{ij} = \varepsilon_{ij} + \omega_{ij}$), representing the strain and rotation effect respectively. The first matrix ($\varepsilon_{ij} = (u_{ij} + u_{ji})/2$), symmetric, is the internal deformation while the second one ($\omega_{ij} = (u_{ij} - u_{ji})/2$) is a whole-body rigid motion. The strain tensor diagonalization led to eigenvectors and eigenvalues which satisfy the relation $\mathbf{E}\bar{v}_k = \lambda_k \bar{v}_k$ (k = 1, 2), providing the diagonal matrix $\mathbf{Ed}$, in which $\mathbf{Ed}_{kk} = \lambda_k$, by means of the transformation $\mathbf{Ed} = \mathbf{V}^{-1}\mathbf{EV}$ (Arfken, 1985; Wolfram, 2006): the columns of $\mathbf{V}$ are the two eigenvectors, that is $\mathbf{V} = [\bar{v}_1 \quad \bar{v}_2]$. In the next the eigenvalues will be named e_{max} and e_{min} following the usual geophysical notation. In this new reference system no shear deformation is present and variations occur along the principal axes only. Taking into account the time dependence, using velocity data instead of displacements and the velocity gradient tensor instead of the displacement one, the same formula allow to define the strain rate (that is the strain for unit time).

Going from continuous to discrete and from theory to application, using sparse velocity vectors estimated at each station of a GPS network, the equations become $u_{i(n)} = L_{ij}\Delta x_{j(n)} + U_i$, where $\Delta x_{j(n)} = (x_{j(n)} - x_{j0})$, x_{j0} is the coordinate of a reference point (for example the centre of mass) and n means one of the available N velocity data. Under the hypothesis of uniform strain field condition, and solving the redundant equation system with a linear least square inversion, the velocity gradient components are estimated together with their errors; the latter, as known, are obtained from the residuals between estimated values and observed ones. This method allows the determination of only one single value for horizontal deformation tensor in the whole investigated area.

The approach previously described can be applied also over a dense distributed data set to attempt to define a continuous deformation pattern. Considering a regular grid, created by taking into account the points distribution (to define its dimension and characteristics), the estimation for a local strain can be performed over each node but using a suitable weighting strategy to automatically lower the contribution of stations distant from the node. All available data are involved in computation but errors are rescaled using an appropriate function, which increases with distance and is not divergent within a chosen area around the point. Following Shen et al. (2000), who used a similar method to fit a model of continuous deformation, we adopted the weight function $e^{-d/d0}$, where d is the node-point distance and $d0$ is a parameter defined for rescaling (see below). Figure 1 was made to become familiar with the use of this smoothing function: it shows a family of curves in a 100 km range, for different $d0$, and it also suggests that a convenient choice for determining a local strain estimation (selecting observables near the point) can be to relate $d0$ with the mean inter-distance between stations.

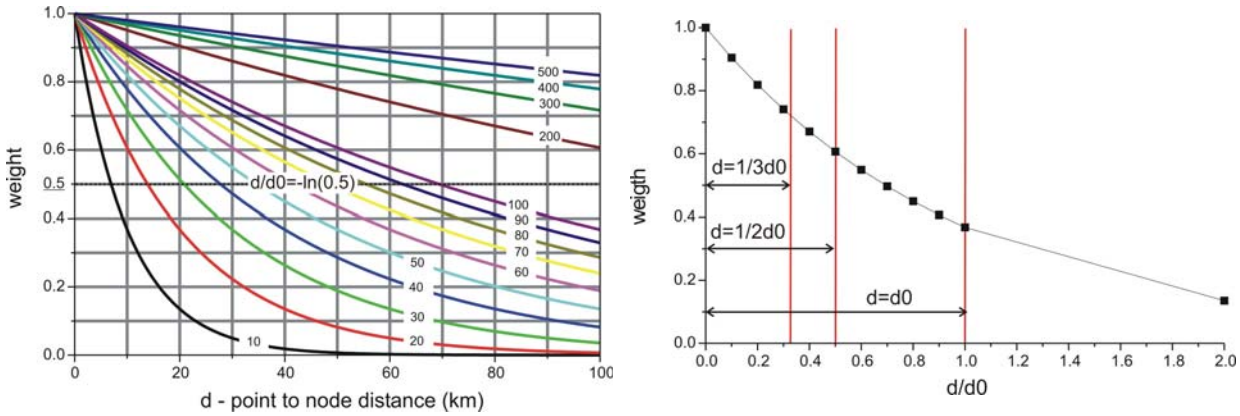

Fig.1 - Weight functions family for different *d0*: values go to zero, increasing the distance between point and node. In particular, at the distance $d = 0.7d0$ the error is doubled.

Fig.2 - The weight function decreases with *d*/*d0* dimensionless distance: in the *d0* around of each node the scaling factor ranges from 1 to about 0.4.

Figure 2 shows the values of weight factors obtained by a few adimensional distances *d*/*d0*: in particular, defining the grid length as the mean of station baselines and *d0* equal to the value of grid length, the points included in the circle area, centred on the node, with radius *d0* are rescaled from 1 to about 0.4 at the distance *d=d0*. Simply speaking, the choice of how local the strain estimation is (and how well the computed values represent local deformation), is performed through *d0*.

The angular distribution of points around each node is very important to ensure the validity of local strain computation; clearly the node has to be included inside a consistent and significant data set after error scaling. In fact, the results obtained on a specified node can be effectively considered only if they are really significant on the basis of error scaling. The method used in this work and implemented in the Matlab™ program is based on a control routine which looks for correct angular distribution of points inside a limited area; this routine operates during computation to detect areas where results could be not representative of a realistic deformation. Both the angular and radial distribution of stations around each node of the grid were used to exclude or accept estimates of the strain. The two-dimensional plane was divided into three equal sectors of 120 degrees and at least one observable was required within each one of these, to satisfy the first acceptance criteria. The radial control checks for node-station distances lower than three times the grid length. This control, added to the weighting strategy used for error rescaling, improves the significance of the strain rate pattern interpretation. The optimal situation is shown in figure 3a, where stations are regularly located around and near the node with respect to the *d0* characteristic distance. In this case, the obtained result is highly significant. Also the situation depicted in figure 3b is acceptable, but the strain evaluated at the node does not have the same local nature of the former, due to longer point distances.

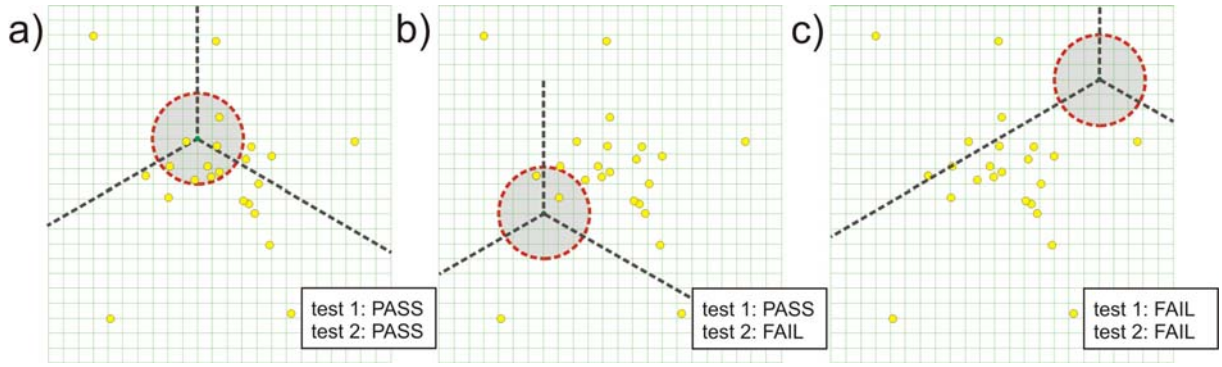

Fig.3 - a) Optimal geometry for test success; b) Good distribution for deformation estimate but at a larger scale (not truly local estimation); c) Point exclusion and estimate removal.

This simple choice of spatial subdivision in three sectors is introduced to accept only points which are included in a relative small polygon, at least in a triangle. A negative situation that leads to the exclusion of the estimation is shown in figure 3c. In this case, the angular distribution is unbalanced and points are too distant from the grid node: the computed strain is therefore devoid of significance.

The approach used for continuous strain determination was applied to a synthetic data set, belonging to a simple planimetric deformation pattern induced by a sphere located at a given depth *f*, with radius *a*, stressing with a ΔP hydrostatic pressure (fig.4) (Mogi, 1958). Maruyama

(1964) provided the analytic solution for the displacement field on the free surface $z = 0$ and we computed its horizontal components as follows in figure 4.

.

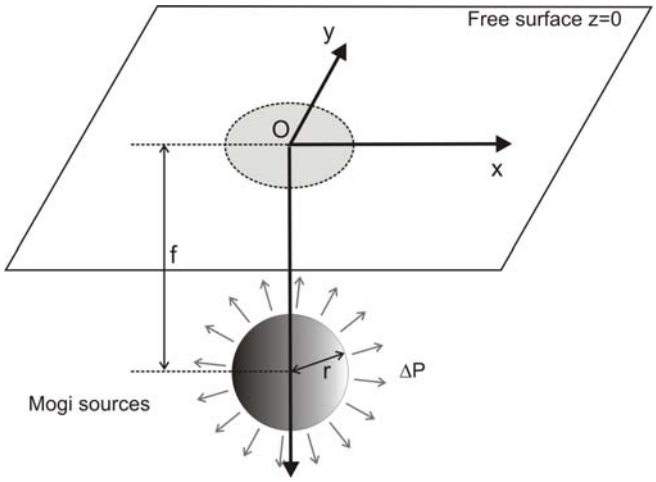

$$u_x = -\frac{C}{\lambda+\mu}\frac{x}{R^3}$$

$$u_y = -\frac{C}{\lambda+\mu}\frac{y}{R^3}$$

$$R = \sqrt{x^2+y^2+(f)^2}, \quad C = -\frac{1}{2}r^3\Delta P$$

$\lambda, \mu = 3\times10^{10}$ Pa	$f = 10000$ m
$\Delta P = 3\times10^{10}$ Pa	$r = 3000$ m

Fig.4 – Analytic formulas for displacement field along the x and y Cartesian axes on the free surface (*z=0*) caused by a sphere of radius *r*, located at the depth *f*, which stresses with a pressure Δ*P*.

The areal distension or shortening over the free surface, due to this kind of model, is computed as the trace of the matrix ($u_{x,x} + u_{y,y}$) and drawn in figure 5 over a 50 km x 50 km horizontal plane, showing a clear radial symmetry.

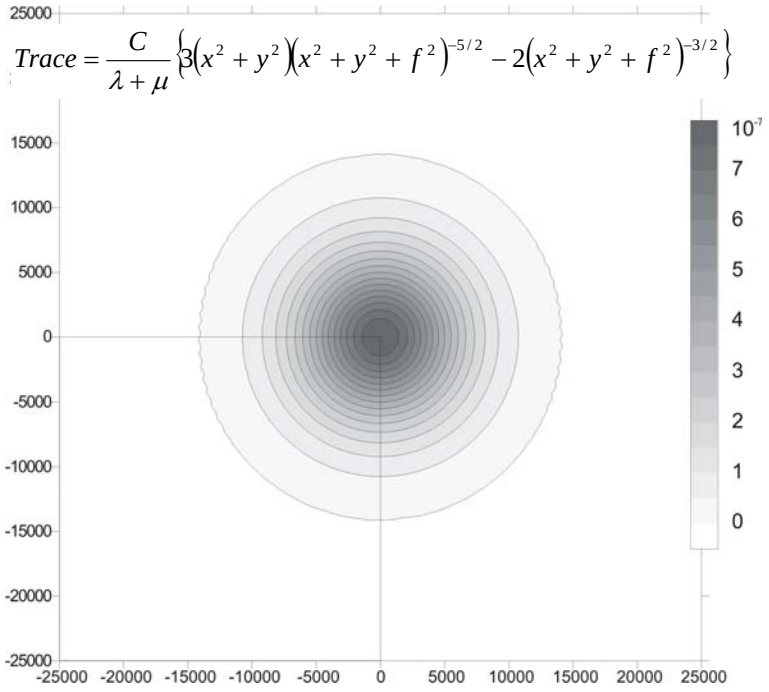

Fig.5 - Theoretical areal deformation: the radial symmetry is evidenced.

Synthetic displacements were computed over a dense and regular distribution of points around the spherical source projection on the surface: the modulus of vectors decreases with the distance from the centre of the plane as shown in figure 6. Respect to the previous figure, the coordinate system was translated to define the origin as (*x=0 and y=0*) ant to deal only with positive coordinates of points. The grey lines of figure 7b represent the grid nodes where the

automatic strain estimation was executed: the grid length and the smoothing parameter *d0* were kept to 2 km.

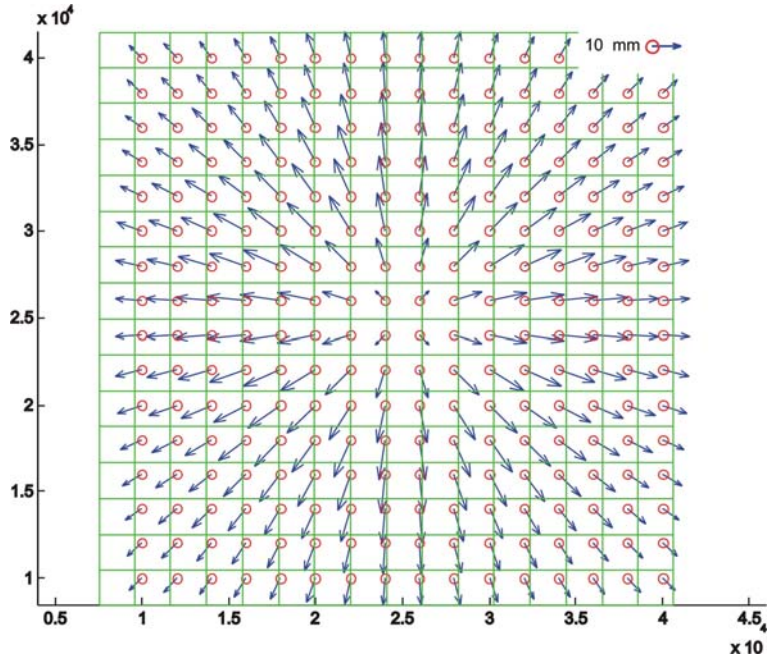

Fig.6 - Synthetic velocity field: vectors were computed over red points well distributed in the area stressed by a Mogi source.

Following the approach above described, the strain tensor was automatically estimated over each node and results are shown in figure 7a: the blue arrows represent the extension while the red ones indicate compressive behaviour. Figure 7b shows the strain trace which is representative of the areal deformation. The red lines represent the theoretical values directly obtained by the *x* and *y* partial derivatives of analytic formulas. In both cases the radial geometry expected by the symmetry of analytical functions is evidenced.

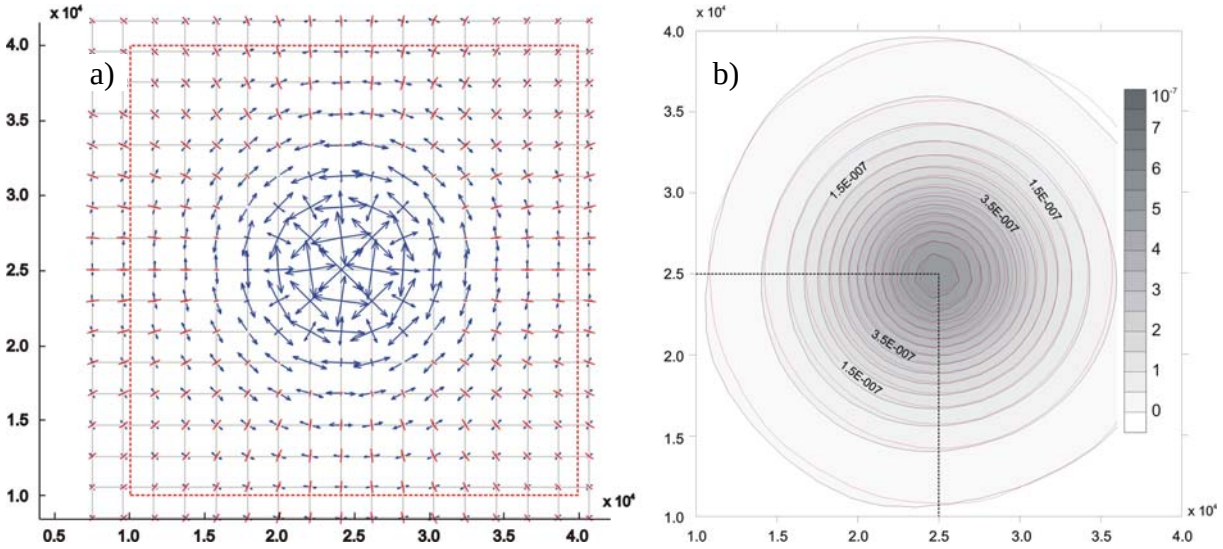

Fig.7 – a) Estimated strain tensor pattern and b) contour lines of both strain trace obtained by discrete data processing (dark lines) and theoretical computation over grid nodes (red lines).

The difference between model and results are also pointed out in figure 8: residuals obtained by direct comparison over the same points are simply analyzed and the mean and the standard deviation of their statistical distribution where computed showing low values.

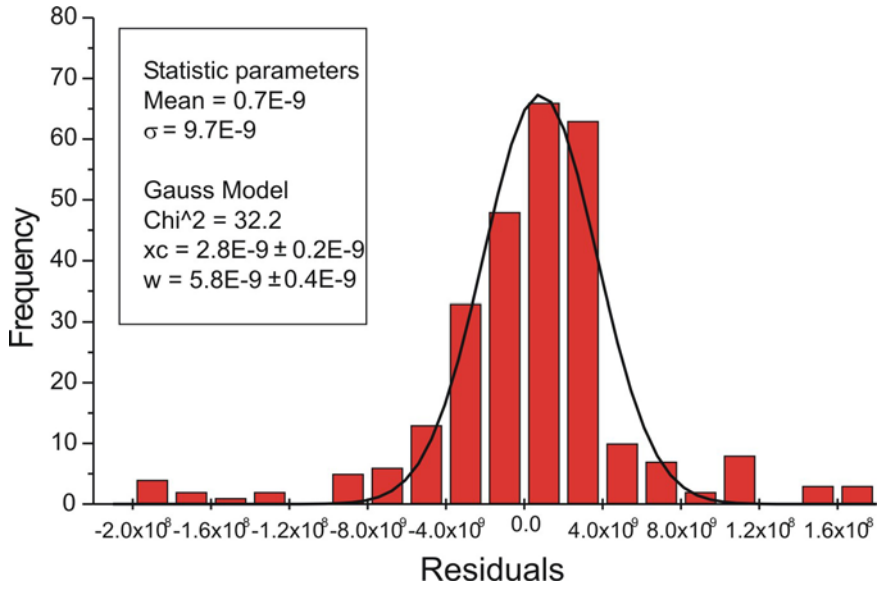

Fig.8 – Residuals between areal deformation computed over the grid nodes and theoretical values. The Gaussian function was estimated showing a small and negligible discrepancy with data.

Despite the agreement between analytic values and local strain estimations, which validate the practical approach adopted, it is necessary to evidence that the point distribution, used in this case, was optimal for computational proposal. The previous example was included in this analysis to prove the correctness of such approach to the strain field determination from discrete data sets. A further experiment is proposed using synthetic data with normal distribution in the same area with high density but irregular geometry. The same Mogi source was used and also the grid length and *d0* factor were kept on the values previously used. The displacements computed on random points are shown in figure 9a while the strain tensor is in figure 9b. In this case the estimates were only accepted on nodes with good geometry distribution and the significant plot is overlapped on data.

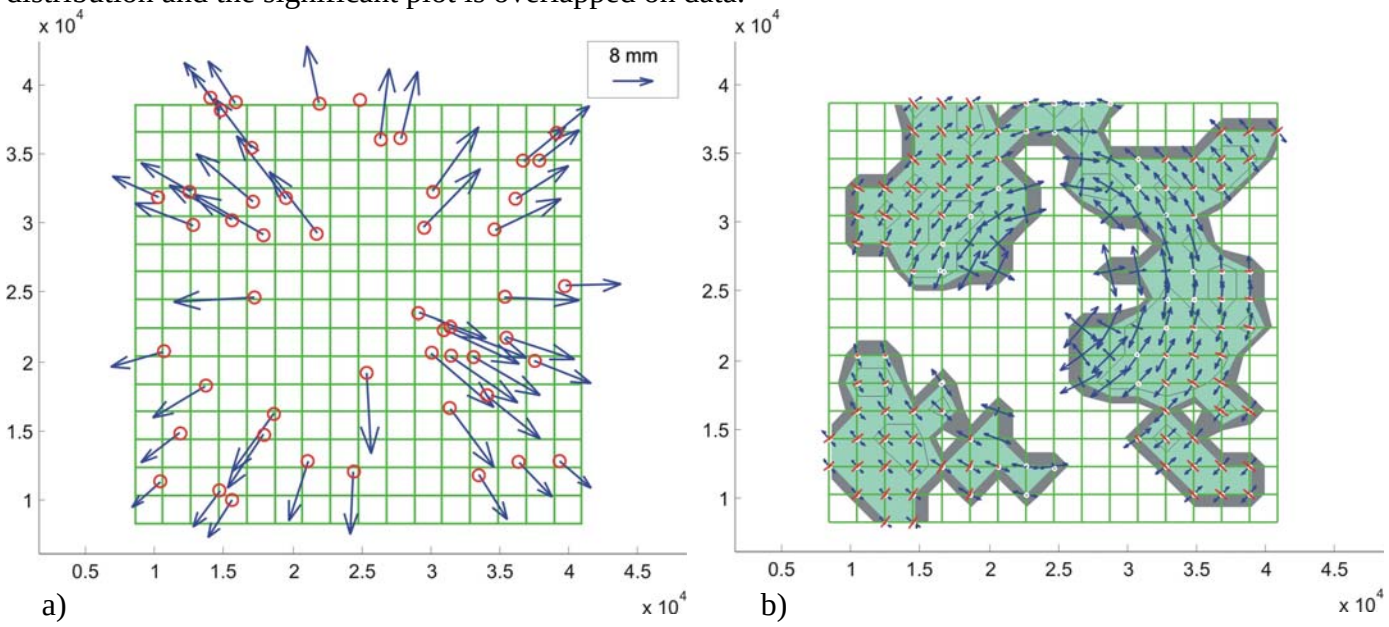

Fig.9 - a) Random point distribution and synthetic velocities; b) strain tensor computation and exclusion of insignificant nodes.

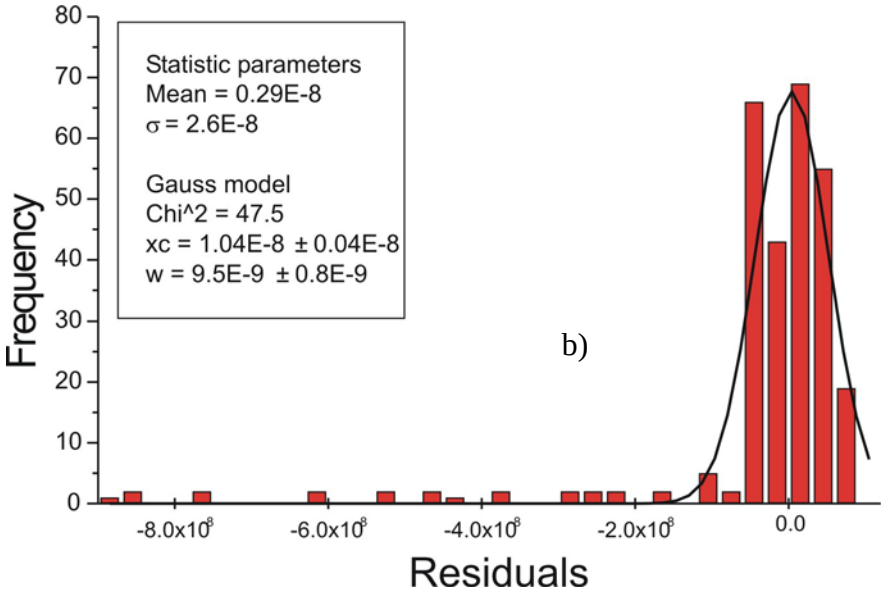

Fig.10 – Residuals distribution analysis: statistic parameters are computed and the Gaussian model fitted by the data.

Despite a dense distribution of points and their almost correct geometry, in this case the observations are not sufficient to model the source precisely: inside the used point distribution, the data gap is mainly in the central part of the area where theoretical values are the larger the complete set. Anyway residuals values are reasonable and the standard deviation is always one order of magnitude lower than expected deformation (10^{-8} vs 10^{-7}).
These simple applications evidence that, even if the approach allows to define significant strain tensors, results cannot be representative of the real deformation pattern, degrading the possibility to detect the model characteristics accurately.
From now on, GPS velocities will be used instead of displacements, introducing a temporal dependence: therefore strain values will concern the deformation for a unit time (or strain rate).

Central Apennine analysis and results

The CAGeoNet (Central Apennines Geodetic Network) was designed to measure both the sub-regional and near-field strain rates across the main seismogenic structures and faults, which are supposed to drive the crustal dynamics of this area. The analysis was performed on velocity data belonging to the network processing over three years of semi-permanent surveying (Anzidei et al., 2006). The strain rate was computed over a regular 10 km x 10 km grid. At each node the areal deformation, given by the tensor trace (sum of eigenvalues), was calculated. The control routine applied during computation allowed the detection of areas where results could not be representative of a realistic deformation. The analysis procedures are explained in the Appenix A together with a complete software description.
Results show a detailed view on the current sub-regional and near deformation field acting in this area, thanks to the high number of stations. Imposing results over a map (fig.11), it is important to point out that the CAGeoNet GPS stations located in the near field across the faulted area, show both extensional and compressive behaviour at the same values, along the chain axis. In particular, the western part of the network is characterized by a compressive regime (negative component of strain tensor) meanly along the EW direction. In the eastern part, on the contrary, there is a clear distension. Red circles are the permanent stations continuously recording GPS data and the red lines compose the polygon which contains the

whole network (measured during the 1999-2003 time span by means of semi-permanent surveys). On figure 11a six grey boxes are evidenced and the strain tensor components, computed at their centre, are reported. Here the pattern variability is shown: values range from the minimum -7.7 10^{-8} to the maximum 8.9 10^{-8} (yr^{-1}). The transition zone seems to be located along the Apennine chain. The tensors trace which represents areal deformation (fig.11b) shows a negative to positive variation exactly perpendicular to the chain: contour lines, in fact, are almost aligned to seismogenic source structures.

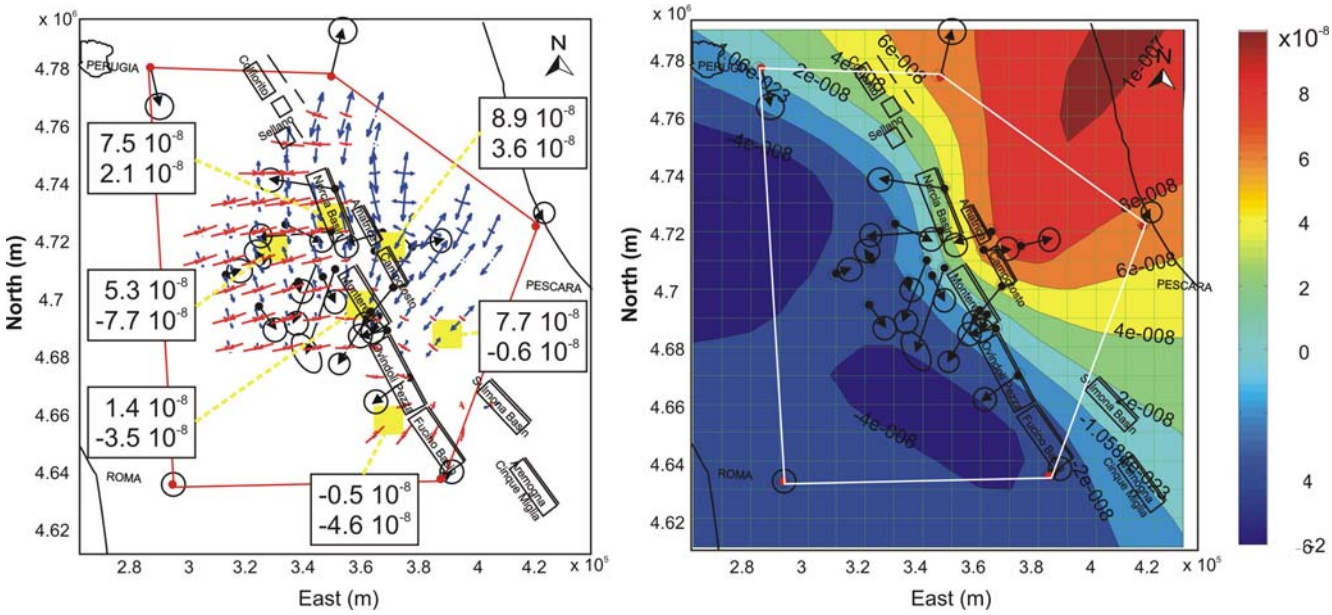

Fig.11 – a) Strain tensors computed over nodes of the regular grid as continuous function: six values are extracted providing internal network deformations; b) areal deformation (tensor trace): a clear inversion from negative to positive values occurs passing through the chain.

Moreover, in figure 12, the two different patterns are evidenced by the normalized values $(e_{max} - e_{min})/(e_{max} + e_{min})$, related to the maximum shear of the area (see Appendix B). Values are quite negative in the western part, where tensor elements have different signs. In the other part, east of the chain, low positive values are computed and the predominance of extension is clearly indicated.

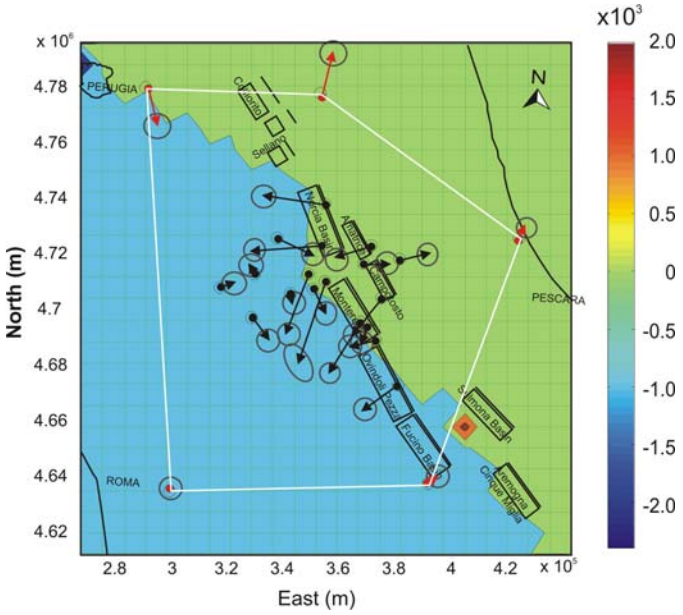

Fig.12 – Maximum normalized shear pattern: also in this case a clear difference between the two regional zones at west (negative) and at east (positive) of the chain is evidenced.

In a previous study (Anzidei et al., 2005) the mean strain, computed using permanent stations only, led to e_{max} and e_{min} values of 1.6 10^{-8} and -1.4 10^{-8} respectively. Other previous geodetic studies estimated maximum strain for the Central Apennines at 1.8 x 10^{-8} (D'Agostino et al. 2001), 5.7 x 10^{-8} (Caporali et al., 2003), from 0.4x10^{-8} to 11.6 x 10^{-8} (Hunstad et al., 2003), 0.4 x 10^{-8} (Ward, 1994), 3.1x 10^{-8} (Serpelloni et al., 2002), with similar orientations with respect to those shown in this paper.

Conclusions

The principal features of a new original scientific software conceived for the strain rate (or strain) estimation on a regular grid using velocity (or displacement) data provided by a series of GPS stations were presented. The software, `grid_strain`, provides the intensity and direction of principal components of strain tensor in each point of the grid, as well as the significance of obtained results on the basis of spatial distribution and accuracy of available measurements. The development of this software allowed a detailed analysis of GPS velocity data in the central Apennine of Italy, where a dense network was established a few years ago. The network grid at 3-5 km, which is optimal with respect to the average seismogenic fault size for the central Apennine, allowed the revealing of new features for this region which can be in agreement with kinematics produced by a retreating subduction and its deepening in the mantle. While the *regional* geodetic network of permanent stations (CGPS stations) provides deformation trends that are in agreement with results published in previous papers (see above), the CAGeoNet GPS stations located in the near field across the faulted area, also show a compression at the same level of the extension values along the chain axis. This result can be due to the presence of active faults that drive a NW-SE compression. This is in agreement with (Bigi et al.,2004) that suggests that the Apennine can be subjected to simultaneous extension and compression caused by the still active subduction of the Adria plate beneath the chain. The extensional behaviour of the area is also in agreement with the distribution and trend of the main seismogenic sources reported in Valensise and Pantosti (2001) that could play a major role in the observed deformations and in the kinematics of the Italian peninsula.
This is the first estimate of a simultaneous active crustal compression and extension across the central Apennine that can be due to the elastic accumulating deformation on the faults.

Notes

The `grid_strain` software is available (free) to the scientific community by contacting via e-mail pesci@bo.ingv.it or giordano.teza@unipd.it, who are interested in developing new collaborations. The 3D version of the program will be available in short time.

Acknowledgment

Authors would like to thank Marco Anzidei who projected and realized the CAGeoNet geodetic network allowing the in-depth study of the deformation acting in this complex area.
A special thanks to Fabiana Loddo for the precious assistance during data processing.
A great thanks to Lydia Gulick for her help in correcting the translation from Italian.

References

Anzidei, M., Baldi, P., Pesci, A., Esposito, A., Galvani, A., Loddo, F., Cristofoletti, P., Massucci, A. and Del Mese, S. (2005) - Geodetic deformation across the central apennines from gps data in the time span 1999-2003 - Annals of Geophysics, vol.48, n.2.

Anzidei, M., Pesci, A., Baldi, P. (2006) - new insights on the active strain field of the central apennines (italy) from gps data in the time span 1999-2003 – Geophysical Journal International – under submission.

Arfken, G. (1985): Mathematical Methods for Physicists, 3rd ed. Orlando, FL: Academic Press, pp. 217-229. (http://mathworld.wolfram.com/MatrixDiagonalization.html)

Bigi, S., Costa Pisani, P., Milli S., Moscatelli, M. (2004) - Active thrust front/foredeep depocenter migration vs flexure migration: the evolution of Central Apennines. Submitted to the 32nd International Geological Congress, Firenze 2004.

Caporali, A., Martin, S., Massironi, M. (2003) - Average strain rate in the Italian crust inferred from a permanent GPS network - II. Strain rate versus seismicity and structural geology. Geophys. Journal International, 155, 254-268.

D'agostino, N., Giuliani, R., Mattone, M., and Bonci, L. (2001) - Active crustal extension in the central Apennines (Italy) inferred from GPS measurements in the interval 1994-1999. Geophys. Res. Lett., 28,10,2121-2124.

Hunstad, I., Selvaggi, G., D'agostino, N., England, P., Clarke, P. and Pierozzi M. (2003): Geodetic strain in peninsular Italy between 1875 and 2001 Geophysical Research Letters, 30, (4), 1181.

Koch, K.R. (1988): Parameter estimation and hypothesis testing in linear models, Springer, Berin Heidelberg New York.

Lay, T. And Wallace T.C. (1995): Modern Global Seismology, Academic Press, pp. 34-50.

Maruyama, T. (1964): Statistical elastic dislocations in an infinite and semi-infinite solid, Bull. Earthq. Res. Tokyo Univ., 42, 289-368.

MATHWORKS (2004):

web site http://www.mathworks.com/access/helpdesk/help/helpdesk.html (last access: 01.02.06)

Mogi, K. (1958): Relation between the eruptions of various volcanoes and the deformation of ground surfaces around them, Bulletin of the Earthquake Research Institute (University of Tokyo), 36, 99–134.

Serpelloni, E., Anzidei, M., Baldi, P., Casula, G., Galvani, A., Pesci, A. and Riguzzi, F.(2002): Combination of permanent and non-permanent GPS networks for the evaluation of the strain-rate field in the central Mediterranean area. Bollettino di Geofisica Teorica ed Applicata, Vol.43, n.3-4, 195-219

Shen, Z.-K., And D. D. Jackson (2000): Optimal estimation of geodetic strain rates from GPS data, *EOS Trans. AGU*, 81, No.19, p.S406.

Valensise, L. and Pantosti, D. (2001): Database of Potential Sources For Earthquakes Larger Than M=5.5 in Italy. Annali di Geofisica, vol.44, suppl.1, with CD-ROM.

Ward, S.N. (1994): Constraints on the seismotectonics of the Central Mediterranean sea from Very Long Baseline Interferometry . Geohys. Jour. International, 117, 441-452.

WOLFRAM (2006): web site http://mathworld.wolfram.com/MatrixDiagonalization.html (last access: 01.02.2006)